Anomalous anisotropic magnetoresistance in epitaxial Fe_3O_4 thin films on MgO(001)

R. Ramos, S. K. Arora, and I. V. Shvets
Centre for Research on Adaptive Nanostructures and Nanodevices (CRANN), School of Physics, Trinity College Dublin, Dublin 2, Ireland

(Received 12 August 2008; revised manuscript received 22 October 2008; published 1 December 2008)

Studies of the angular dependence of the anisotropic magnetoresistance (AMR) are reported for epitaxial films of magnetite (Fe_3O_4) grown on MgO(001) and also for single crystals of magnetite. The characteristic feature of the AMR is a twofold symmetry at temperatures above 200 K. As the samples are cooled below 200 K, an additional set of peaks appears. These become dominant at lower temperatures showing an overall fourfold symmetry. Observation of additional anisotropy in the AMR points to formation of charge ordering at much greater temperatures than the Verwey transition temperature and is possibly related to the polaron formation in magnetite.

DOI: 10.1103/PhysRevB.78.214402 PACS number(s): 75.47.−m, 75.50.Bb, 71.30.+h

I. INTRODUCTION

Many transition-metal oxides exhibit charge and orbital orderings which manifest themselves in a spatial localization of charge carriers on certain ionic sites and electron orbitals, respectively. These correlated ordering processes govern the physical properties, such as magnetism and charge transport, and are responsible for many ubiquitous phenomena.[1–3] Magnetite, Fe_3O_4, is one of the important 3*d* transition-metal oxides due to its half metallic nature, high Curie temperature (858 K), and presence of a metal-insulator transition (MIT) at around 121 K (known as Verwey transition). Hence, it is viewed as a potentially interesting material for spintronic applications.[4,5] The Verwey transition in Fe_3O_4 leads to a change in conductivity by 2 orders of magnitude across the transition temperature and is believed to be associated with a order-disorder transition from a charge-ordered state of *B*-site Fe ions ($Fe^{+2,+3}$, for octahedral Fe ions) at low temperatures to a disordered state ($Fe^{+2.5}$ at all *B* sites) at higher temperatures. Despite decades of activity, the underlying physics related to this transition is not yet completely clear.[6] Various techniques have been used to grow epitaxial heterostructures based on magnetite. MgO is an ideal template to grow Fe_3O_4 films owing to the small lattice mismatch.[7–10] However, the Fe_3O_4/MgO heteroepitaxial system suffers from the formation of antiphase boundaries (APB) which is an innate outcome of the growth process due to the fact that Fe_3O_4 has a unit cell which is twice the size and lower in symmetry compared to MgO.[7–10] The presence of APBs has a deleterious effect on the magnetic properties but they are beneficial in enhancing the magnetoresistance of films due to additional spin scattering they induce.[11,12] Magnetotransport studies in epitaxial magnetite films are mostly focused on the influence of APBs, disorder, and strain. In a recent study,[13] we showed that if these nanoscale defects in Fe_3O_4 films are manipulated in an ordered fashion one can attain a sizable magnetoresistance.

Understanding mechanisms that affect the magnetotransport behavior in Fe_3O_4 is of crucial importance in realization of its application as a magnetoresistive sensor. One of the mechanisms contributing to the magnetotransport phenomenon is the anisotropic magnetoresistance (AMR). In ferromagnets, the AMR is caused by the spin-orbit interaction, which induces the mixing of spin-up and spin-down states.[14–16] This mixing depends on the magnetization direction and gives rise to a magnetization-direction-dependent scattering rate. As a result, the conductivity of a saturated sample is affected by the angle between the electrical current $\vec{J}$ and magnetization $\vec{M}$. The angular dependence of resistivity is given by

$$\rho = \rho_{\perp} + (\rho_{\parallel} - \rho_{\perp})\cos^2\theta, \tag{1}$$

where $\rho_{\parallel}$ and $\rho_{\perp}$ are the resistivities for $\vec{M} \parallel \vec{J}$ and $\vec{M} \perp \vec{J}$, respectively. Various mechanisms have been proposed to explain the origin of the AMR and its link to spin-orbit coupling. Some aspects of AMR were dealt theoretically by Smit,[14] Berger,[17] Potter,[18] and Campbell *et al.*[19] In ferromagnetic polycrystalline alloys the magnitudes of the AMR are around 20% and 5% at low temperature (20 K) and room temperature, respectively. In thin films, its magnitude is further reduced due to surface scattering and additional structural effects. In single crystals and epitaxial thin films, in contrast to polycrystals, additional features in AMR at low fields are observed which are related to the magnetocrystalline anisotropy and the AMR exhibits a deviation of the angular dependence from the $\cos^2\theta$ curve.[20,21] Enhanced magnitude of up to several tens of percent could be obtained in nanostructured devices such as multilayers, constrictions in the ballistic regime, and nanowires.[22,23] There are studies aimed at understanding the charge and spin coupling on AMR. In particular, AMR investigations in epitaxial thin films and single crystals of rare-earth manganites have shown an anomalous temperature dependence where the magnitude of AMR peaks at a temperature close to the MIT, which is an issue actively debated by theoreticians and experimentalists.[24,25] In Fe_3O_4 films, the AMR investigations were performed by Ziese and Blythe.[26] In films of thickness larger than 15 nm, they found a temperature-independent AMR ($\sim$0.5%) for $T > 200$ K and a sign change in AMR at temperatures close to Verwey transition. No details of the angular dependence of the AMR were provided.

In this paper we report a detailed study of angular and temperature dependences of AMR in a synthetic single crys-

tal of Fe_3O_4 and epitaxial Fe_3O_4 films of different thicknesses grown on MgO(001) substrates. Remarkably, in angular dependence of AMR, we observe an additional anisotropy, superimposed on the conventional twofold anisotropy at temperature below 200 K. Its magnitude grows with an increasing field and decreasing temperature. We provide possible explanations for the observed effect.

II. EXPERIMENT

The Fe_3O_4 thin films of thicknesses 33, 67, and 200 nm were grown on MgO(001) single-crystal substrates using an oxygen-plasma-assisted molecular-beam epitaxy (DCA MBE M600) with a base pressure of 5×10^{-10} Torr. The substrates were annealed at 600 °C in UHV for 1/2 h followed by 2 h annealing in 1.1×10^{-5} Torr oxygen. The growth of Fe_3O_4 films was carried out by means of electron-beam evaporation of pure metallic Fe (99.999%) in the presence of free oxygen radicals (1.1×10^{-5} Torr). Substrate temperature during growth was 250 °C. Details of the growth procedure can be found elsewhere.[13] Resistance versus temperature measurements for the samples were performed using a standard four-probe method. Prior to the transport measurements, the samples were patterned into the Hall bar geometry by UV-lithography and chemically etched with an 8.55 M HCl solution.

The magnetotransport measurements were carried out using a physical property measurement system (PPMS 6000 system of Quantum Design), which is equipped with a 14 T superconducting magnet and a sample rotator to perform the measurements at different field orientations in a temperature range of 2–400 K. In order to study the angular dependence of the AMR, the samples were subjected to a constant in-plane magnetic field $\vec{H}$, while the angle θ, with respect to the electric current I, was changed from 0° to 360°. The longitudinal voltage which is proportional to the AMR was measured between contacts V^+ and V^- [inset of Fig. 2(a)]. A dc bias current was applied along the ⟨100⟩ direction, the applied current was always kept in 1–10 μA range for the thin-film samples and in 1–10 mA range for the single crystal, and the I-V characteristics of the studied samples exhibited linear behavior for the electrical currents used in the AMR experiment for all the temperatures measured. The synthetic crystal of Fe_3O_4 used in this study was grown employing the skull-melting technique and showed a Verwey transition temperature of 119 K.

III. RESULTS AND DISCUSSION

We present a systematic study of the angular dependence of the anisotropic magnetoresistance at different temperatures and magnetic-field strengths on 33, 67, and 200 nm thick Fe_3O_4 films grown on MgO(001) substrates. Prior to the AMR measurements the temperature dependence of the resistivity was measured. Figure 1(a) shows the resistivity as a function of temperature for all the films. Also shown in the figure is the data for a single-crystal slice of Fe_3O_4 cut along the (001) plane. Resistivity of the films at 300 K is found to increase with a decrease in film thickness and is greater than

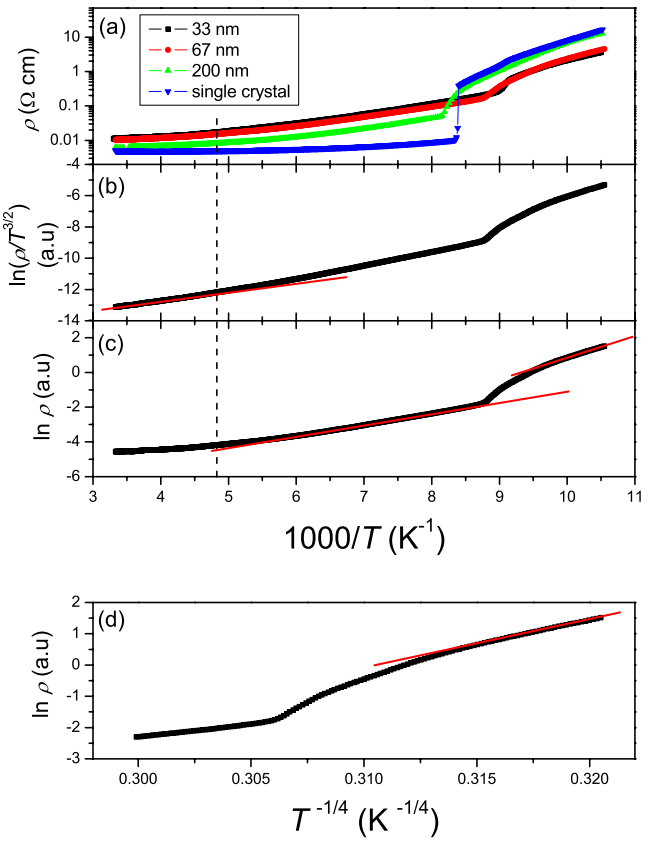

FIG. 1. (Color online) (a) Temperature dependence of the resistivity for all the thin-film samples of Fe_3O_4 along with that of single-crystal Fe_3O_4 samples. The Verwey transition temperatures are found to be 110, 112, and 121 K for the 33, 67, and 200 nm thick films, respectively. Verwey transition for the single crystal was 119 K. Panels (b)–(d) show the resistivity of the 67 nm thick film fitted (red lines) to the (b) small-polaron hopping, (c) Arrhenius law, and (d) variable-range hopping (VRH) models. The VRH expression is only fitted for temperatures below T_V.

that of the single crystal. Verwey transition temperature (T_V) for 33, 67, and 200 nm films is found to be 110, 112, and 121 K, respectively. These observations are in line with the previously reported values of resistivities and T_V.[26,27] Temperature dependence of resistivity for Fe_3O_4 films suggests that the electronic transport in Fe_3O_4 follows a thermally activated behavior. As previously reported,[28] three regions with different activation energies can be distinguished. The first one is a high-temperature region ($T\gtrsim200$ K), the second is a middle temperature region (just above T_V up to ~200 K), and the third a low-temperature region (below T_V), hereafter referred to as regions I, II, and III, respectively. In order to understand the mechanism of charge transport in Fe_3O_4, we fitted the resistivity data using expressions for small-polaron hopping [$\rho/T^{3/2}=A\exp(W_p/k_BT)$] in region I, Arrhenius law or band-gap model [$\rho=\rho_\infty\exp(E_a/k_BT)$] in regions II and III, and variable-range hopping [$\rho=\rho_\infty\exp(T_0/T)^{1/4}$] for temperatures below T_V.[29] Figures 1(b)–1(d) show the data for the 67 nm thick film fitted to small-polaron hopping [Fig. 1(b)], Arrhenius law [Fig. 1(c)], and variable-range hopping [Fig. 1(d)]. From the slope of the curves we obtain the polaron hopping energy (W_p), activation energy (E_a), and Mott tem-

TABLE I. Values of activation energies (E_a) and polaron hopping energies (W_p) at 0 T in different temperature regions determined using various conductivity models for different thickness films and single-crystal magnetite. W_p^I relate to the temperature region $T>200$ K; E_a^{II} to the region 120 K$<T<$200 K. E_a^{III} and T_0 were obtained at temperatures below the Verwey transition.

Thickness (nm)	Arrhenius law (meV) $\rho=\rho_\infty \exp(E_a/kT)$		Small-polaron hopping (meV) $\rho/T^{3/2}=A\exp(W_p/kT)$	VRH (K) $\rho=\rho_\infty \exp(T_0/T)^{1/4}$
	E_a^{II}	E_a^{III}	W_p^I	T_0 (regime III)
33	58.0	92.5	53.0	3.7×10^8
67	56.8	102.9	52.6	6.0×10^8
200	55.0	106.9	46.1	8.8×10^8
Single crystal	31.8	112.6	33.0	9.1×10^8

perature (T_0), respectively. These parameters obtained using the above models are summarized in Table I. The values of E_a agree well with previous reports[26] both above and below T_V. The Mott temperature T_0 is found to be related to the localization length[30] and agrees well with earlier reported values.[31] The existence of two different electrical conduction regions above T_V (i.e., *regions I and II)* in magnetite agrees well with the model of Ihle and Lorenz[32] for small-polaron (SP) band and SP hopping conduction, the first one being dominant at lower temperatures (just above T_V, region II) and the latter one at higher temperatures (region I).

Now, let us examine the temperature and magnetic-field dependence of the measured AMR. The AMR is usually defined as the ratio AMR$=(\rho_\parallel-\rho_\perp)/\rho_{\text{ave}}$, where $\rho_\parallel$ and $\rho_\perp$ are the resistivities for magnetic field applied parallel and perpendicular to the current direction, respectively, and $\rho_{\text{ave}}=\rho_\parallel/3+2\rho_\perp/3$. Our results show a room-temperature value of about 0.3%, in agreement with earlier reports.[26,33,34] Figure 2(a) shows the relative amplitude of the angular dependence of the magnetoresistance for the 67 nm sample at an applied field of 5 T for a series of temperatures $T=300$, 250, 200, 150, and 120 K (defined as $\Delta\rho/\rho_{\min}(\%)=[(\rho(\theta)-\rho_{\min})/\rho_{\min}]\times100$, where θ is the angle between magnetic field and current and $\rho_{\min}$ is the minimum of resistivity for each scan). The data were also taken in the reverse angular sweep and resulted in no hysteresis in the AMR. At high temperatures (above 200 K), the angular dependence of AMR follows the typical $\cos^2\theta$ dependence (twofold symmetry) with peaks at 0° and 180° and valleys at 90° and 270°, respectively. When the sample is cooled down to a temperature below 200 K a deviation from the twofold symmetry starts to appear with the valleys near 90° and 270° broadening and eventually an additional set of peaks appearing showing an overall fourfold symmetry, which becomes dominant at lower temperatures. Similar behavior was exhibited by a (001) oriented stoichiometric Fe_3O_4 single crystal [Fig. 2(b)]. Similar features in the angular dependence of AMR have been previously observed in manganites[35] and more recently in diluted magnetic semiconductors (DMS).[36,37] In the latter case it has been related to the existence of two conduction mechanisms with different temperature dependencies. In general, additional anisotropy terms in the AMR response appear for single crystalline thin films provided the magnitude of external field is below the aniso-

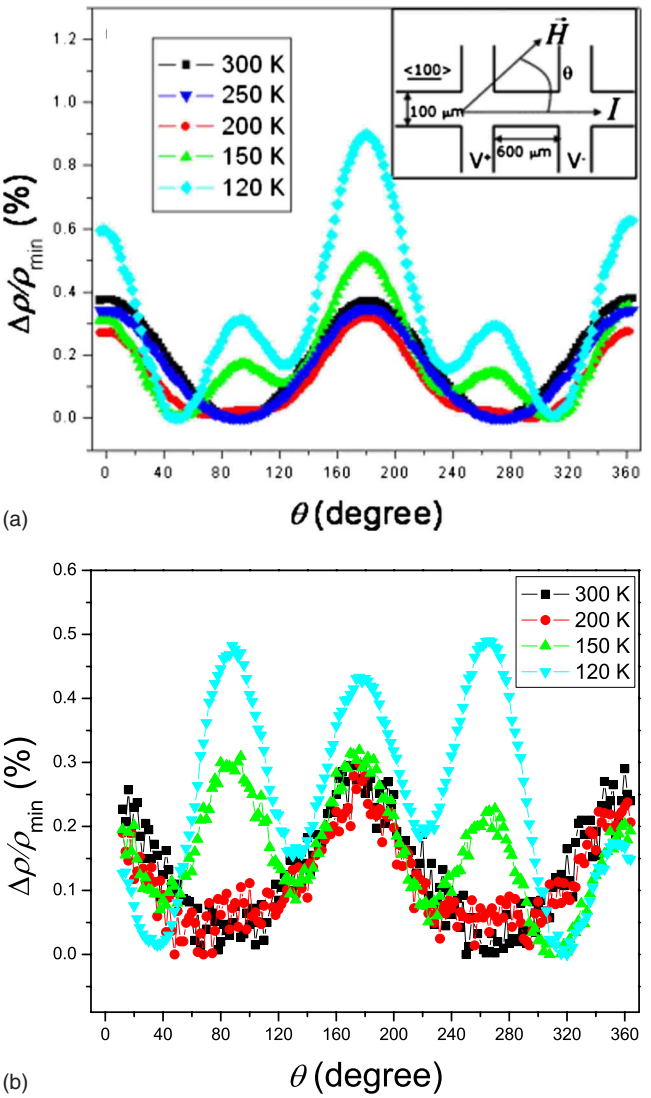

FIG. 2. (Color online) (a) Angular dependence of the magnetoresistance for the 67 nm Fe_3O_4 thin-film sample measured at $\mu_0\vec{H}=5$ T. Below 200 K, it can be seen that the additional anisotropy develops with peaks at 90° and 270°. (b) Angular scan of AMR at different temperatures for the (001) oriented single crystal Fe_3O_4 measured at 5 T field. Inset in Fig. 2(a) shows the Hall bar geometry used in these investigations.

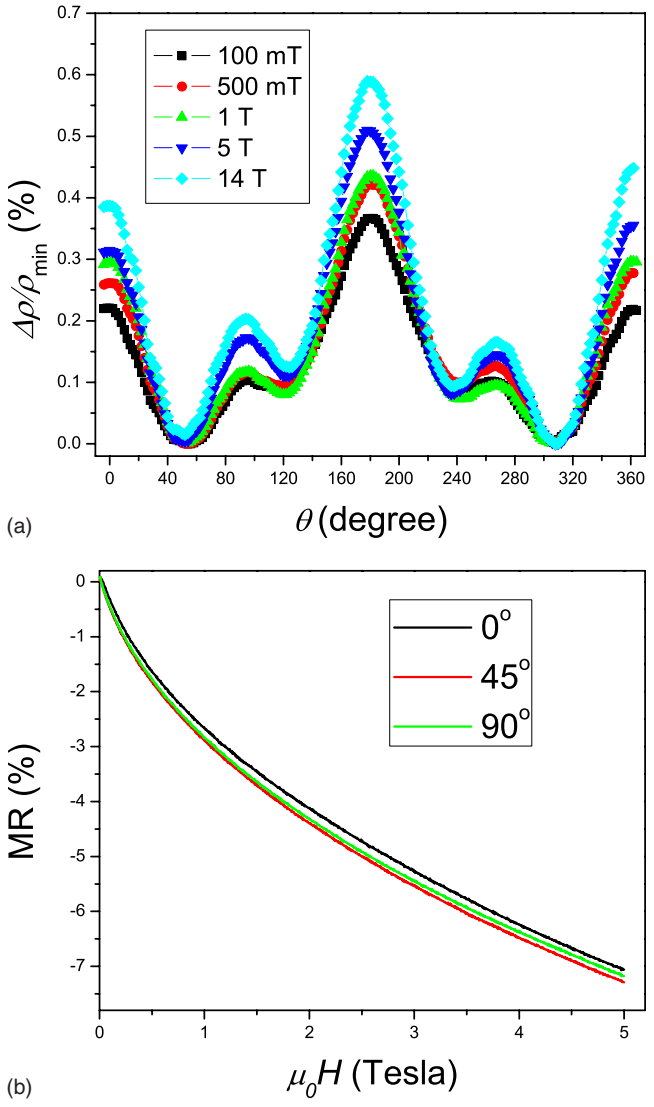

FIG. 3. (Color online) (a) Angular dependence of the magnetoresistance for the 67 nm thick Fe_3O_4 thin film measured at 150 K. The data are plotted for different field values of 100 mT, 500 mT, 1 T, 5 T, and 14 T. (b) Magnetoresistance of the 67 nm thick film measured at field orientations 0°, 45°, and 90° with respect to the current.

tropy field; such an example can be found for the case of a manganite thin film.[38] Besides the additional anisotropy terms arising from the magnetocrystalline anisotropy, they also observed appearance of hysteresis in angular dependence at small fields and low temperatures and attributed it to magnetic inhomogeneities.

The appearance of an additional anisotropy in the AMR in Fe_3O_4 films is quite surprising. In order to establish its possible origin, we investigate the angular dependence of AMR at different magnetic fields. A representative data of angular scans for a 67 nm thick Fe_3O_4 film measured at 150 K with varying magnetic-field strengths (0.1, 0.5, 1.0, 5.0, and 14 T) are shown in Fig. 3(a). Surprisingly, we notice that even with an increase in the magnetic field up to 14 T, we could not overcome this anisotropy. Furthermore the fact that the peaks related to the additional anisotropy are present at positions where the angle between the magnetic field and current is 90° could suggest that it originates because of the contribution of Lorentz force (whose magnitude is greatest when the field is applied perpendicular to the current). The Lorentz force related contribution can be observed if $\omega_c\tau > 0.1$, where ω_c is the cyclotron frequency ($\omega_c = eB/m^*c$) and τ is the scattering time. This condition can be written as $BR_H/\rho = \tan\theta_H > 0.1$, where R_H is the Hall coefficient and θ_H is the Hall angle. For a 5 T field we estimate a value of $BR_H/\rho = \tan\theta_H \sim 10^{-5}$, therefore, Lorentz force effects can be ruled out. Furthermore the magnetoresistance $(\mathrm{MR}(H)(\%) = \{[\rho(H) - \rho(0)]/\rho(0)\} \times 100)$ of the samples is always negative [see Fig. 3(b)], in contrast to the positive magnetoresistance expected from the Lorentz force effects.

In order to understand the mechanism related to this additional anisotropic terms in AMR behavior of magnetite, we need to look at the details of the origin of AMR in ferromagnets. Phenomenologically, AMR shows a twofold symmetry for polycrystalline materials because the magnetocrystalline effect is averaged out. However in single crystals and epitaxial films, it contains higher order terms which reflect the symmetry of the crystals.[39,40]

Using the phenomenological description for the anisotropic magnetoresistance, the dependence of the resistivity tensor with respect to the angle between magnetization and current can be calculated. Expanding the resistivity tensor as a function of the direction cosines of the magnetization and considering the symmetric part only gives

$$\rho_{ij}(\vec{\alpha}) = a_{ij} + a_{ijkl}\alpha_k\alpha_l + a_{ijklmn}\alpha_k\alpha_l\alpha_m\alpha_n + \ldots, \qquad (2)$$

where a_{ij}, a_{ijkl}, a_{ijklmn} are elements of the tensor up to the fourth order and the α_k are the direction cosines of the magnetization. The number of coefficients can be reduced considering the Onsager relation $[\rho_{ij}(\vec{\alpha}) = \rho_{ij}(-\vec{\alpha})]$ and symmetry of the crystal.[41] For an in-plane magnetization and current applied in the $\langle 100\rangle$ direction, the obtained resistivity tensor looks as follows:

$$\rho(\theta) = C_0 + C_2\cos^2\theta + C_4\cos^4\theta, \qquad (3)$$

with $C_0 = a_{11} + a_{1122} + a_{111122}$, $C_2 = a_{1111} - a_{1122} - 2a_{111122} + a_{112211}$, $C_4 = a_{111111} + a_{111122} - a_{112211}$, and θ the angle between magnetization and current directions. This result is based on power expansions in terms of $\cos^n\theta$ even though our data are analyzed using the following expression:

$$\rho(\theta) = a_0 + a_u\cos 2\theta + a_c\cos 4\theta, \qquad (4)$$

since we can extract direct information on the uniaxial and cubic components of the anisotropic magnetoresistance. The a_0, a_u, and a_c constants are related to the previous ones by $a_0 = C_0 + C_2/2 + 5/8C_4$, $a_u = (C_2 + C_4)/2$, and $a_c = C_4/8$.

We fit the angular dependence of AMR using the expression of Eq. (4), obtaining the coefficients a_u and a_c, which are proportional to the uniaxial and cubic components, respectively. These are plotted as a function of temperature for the three different samples and an applied field of 5 T in Fig. 4. It can be noticed that the uniaxial component (a_u) shows a nonmonotonic temperature dependence with its minimum shifted toward lower temperatures with increasing thickness. The cubic component (a_c) shows a monotonic dependence

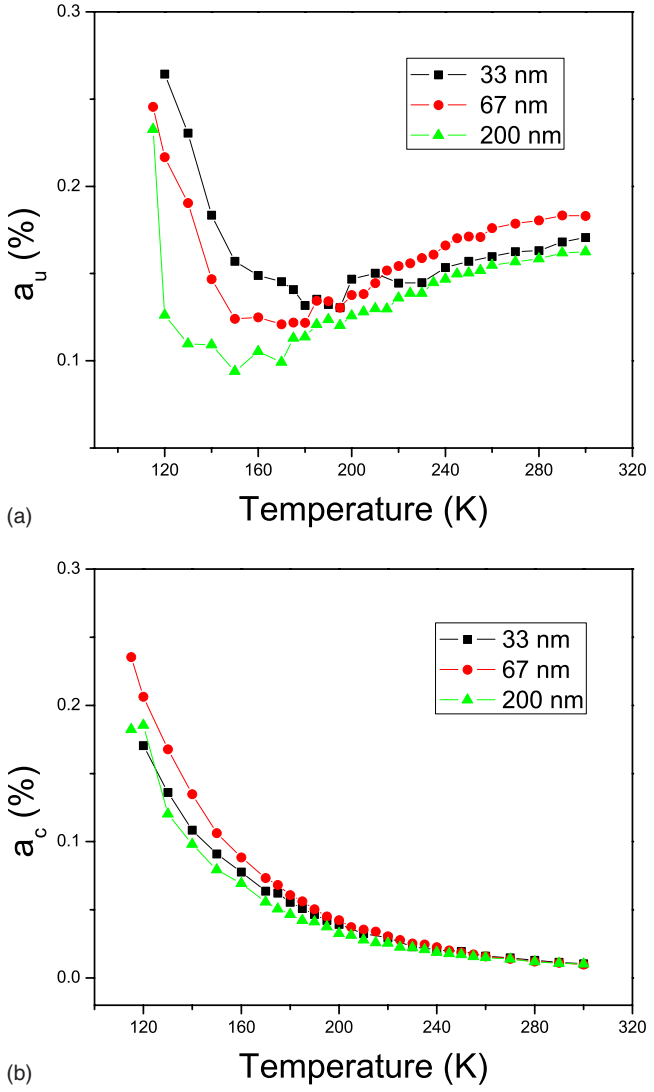

FIG. 4. (Color online) Temperature dependence of the (a) uniaxial (a_u) and (b) cubic (a_c) components for samples of three different thicknesses. The coefficients are determined from the angular-dependent AMR scans taken at each temperature with an applied field of 5 T.

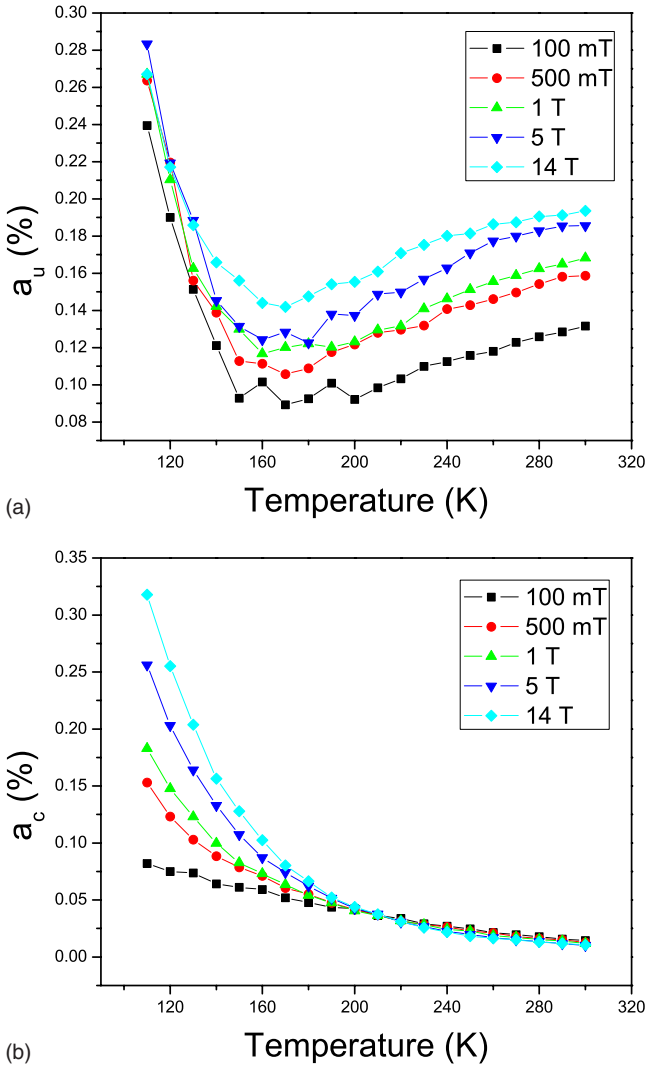

FIG. 5. (Color online) Temperature dependence of the (a) uniaxial (a_u) and (b) cubic (a_c) components at different applied fields for the 67 nm thick film.

with a continuous increase as the temperature is decreased. Wu *et al.*[36] observed a similar behavior in (Ga,Mn)As films. They consider the cubic component arising from the ferromagnetic order of the sample which is due to reduced thermal fluctuations of the spins. As the temperature is decreased and as the spins become more aligned it is possible to observe higher order terms. They considered the uniaxial component to be dependent on the ferromagnetic order as well as on a superparamagnetic component (SPM) arising from bound magnetic polarons (BMPs).

Since the characteristic features are similar for the three thin films, we focus our discussion on the 67 nm thick film sample. Figures 5(a) and 5(b) show the temperature dependence of the fitting coefficients (a_u and a_c) obtained at fields 0.1, 0.5, 1, 5, and 14 T. The uniaxial component shows a similar temperature dependence for all field values. Its magnitude increases with an increasing magnetic field above 140 K. Below 140 K we notice a nonmonotonic field dependence in a_u. The increase in magnitude of a_u with magnetic field for $T > 140$ K is contrary to the notion that AMR [AMR$=(\rho_{\parallel} - \rho_{\perp})/\rho_{\text{ave}}$] is independent of the magnetic field at fields above the saturation field. This behavior can be explained on the basis that Fe_3O_4 films contain APBs, which leads to a field dependent MR due to a nonsaturation of the magnetization in fields up to several Tesla. The nonmonotonic field dependence below 140 K could be related to the sign change of the magnetic anisotropy constant (K_1) in magnetite, which happens above T_V at ~ 130 K.[42] In contrast to it, the cubic component shows the same temperature dependence for all field values and no field dependence down to a temperature of about 200 K. Below 200 K a_c shows a different temperature dependence for different field values with a stronger increase in magnitude for higher magnetic fields. At this moment we do not have a satisfactory explanation for this field dependency.

The fact that the additional symmetry appears at a temperature well above T_V is in agreement with previous reports

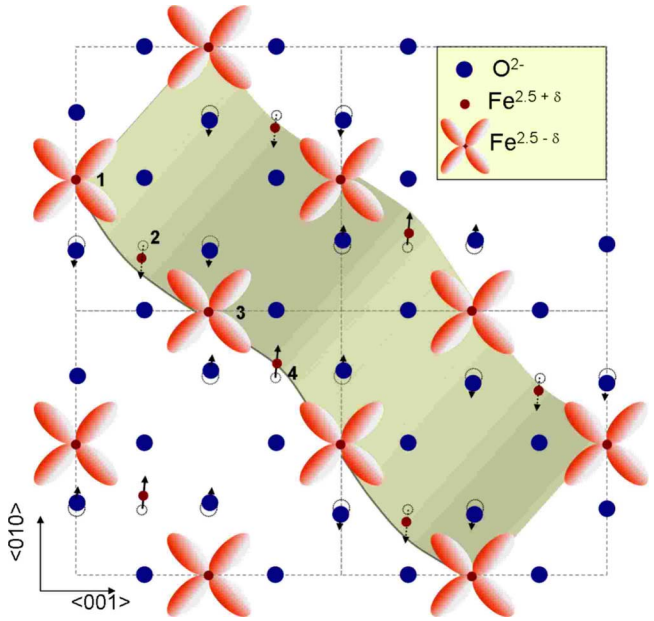

FIG. 6. (Color online) Representation of the atomic displacements induced by the X_3 phonon mode. Broken (solid) arrows represent displacements along $\langle 1\bar{1}0\rangle$ ($\langle\bar{1}10\rangle$). The cations in positions 2 and 4 and their nearest-neighbor anions in the $\langle 001\rangle$ direction are displaced along $\langle 1\bar{1}0\rangle$ ($\langle\bar{1}10\rangle$), respectively, therefore the atomic sites in positions 1 and 3 will present t_{2g} orbital ordering (d_{yz} orbital) due to the lower Coulomb repulsion as a consequence of the out of plane displacement of two of the nearest-neighbor anions.

where anomalies in muon spin rotation (μSR) measurements[43] and neutron-scattering experiments[44,45] have been observed at temperatures $T > T_V + 100$, which have been related to the formation of polarons.

Recalling the discussion on the temperature dependence of the resistivity for our films, we consider the activation energies measured in region II. Following the model by Ihle and Lorenz,[32] the electron-phonon coupling constant (S_0) was obtained and the temperature of transition between the SP band and hopping conduction region was calculated using the expression $kT' = \omega_0\{2\ \ln[2S_0 + (1+4S_0^2)^{1/2}]\}^{-1}$,[46] where $\omega_0 = 0.07$ eV. We obtained the temperature value of $T' = 215$ K for the 67 nm thick film. This is in good agreement with the temperature where the a_c component shows the splitting with the field [see Fig. 5(b)] below some 200 K, suggesting that the observed anomaly is a consequence of a change in the conduction mechanism in magnetite due to the formation of polarons. Piekarz *et al.*[47,48] recently proposed a mechanism for the Verwey transition as a cooperative effect between intra-atomic Coulomb interaction of Fe ions and phonon-driven lattice instability. They developed a model which shows that the strong electron-phonon coupling induces local crystal deformations and a polaronic short-range order above T_V and pointed out that the signs of the metal-insulator transition already appear at about 200 K.[44,45,49] According to their model, the X_3 transversal optic phonon mode is responsible for the observation of charge-order stabilization at temperatures higher than the Verwey transition temperature. This mode consists of atomic displacements of the octahedral Fe and O atoms along $\langle 110\rangle$ and $\langle 1\bar{1}0\rangle$ directions in alternate planes. These displacements modify the interplanar distances between Fe-O atoms, stabilizing charge and orbital order of the t_{2g} states (see Fig. 6). The charge order creates a charge disequilibrium between the Fe ions on B sites (octahedrally coordinated cation sites in the spinel structure of magnetite), ideally departing from the average $Fe^{2.5+}$ state to Fe^{2+} and Fe^{3+} at different octahedral sites. It is known that Fe^{3+} has a singlet ground state $^6S_{5/2}$ with orbital moment zero and therefore no spin-orbit splitting. On the other hand the Fe^{2+} has a ground state $^5D_4$ that will be split by spin-orbit interactions.[50] Therefore the charge ordering produces an enhancement of the effect of the spin-orbit interaction. Since the anisotropic magnetoresistance is a consequence of this interaction[14,15,18] it can be expected that the effect of polaron formation, thus charge ordering in the system, can be observed by anisotropic magnetoresistance measurements as evidenced from our observations.

IV. CONCLUSION

In summary, we performed a study of the angular dependence of AMR for epitaxial Fe_3O_4 films deposited on MgO (001) substrates and also on a (001)-oriented stoichiometric Fe_3O_4 single crystal. It is shown that for temperatures below 200 K, the anisotropic magnetoresistance deviates from its normal $\cos^2\theta$ angular dependence; this deviation is manifested as an additional set of peaks at 90° and 270°. This observation is compared with the mechanism of the Verwey transition suggesting that the additional feature observed is related to a change in the conduction mechanism due to the formation of polaronic short-range order at temperatures above T_V. The effect of polaron formation can be observed by anisotropic magnetoresistance measurements as a consequence of spin-orbit enhancement induced by the charge-order formation as explained above.

ACKNOWLEDGMENTS

Authors would like to gratefully acknowledge the financial support from the Science Foundation of Ireland (SFI) under Contract No. 06/IN.1/I91.

[1] Y. Tokura and N. Nagaosa, Science **288**, 462 (2000).
[2] M. Imada, A. Fujimori, and Y. Tokura, Rev. Mod. Phys. **70**, 1039 (1998).
[3] M. Ziese, Rep. Prog. Phys. **65**, 143 (2002).
[4] I. Žutić, J. Fabian, and S. D. Sarma, Rev. Mod. Phys. **76**, 323 (2004).
[5] M. Fonin, Y. S. Dedkov, R. Pentcheva, U. Rüdiger, and G. Güntherodt, J. Phys.: Condens. Matter **19**, 315217 (2007).
[6] F. Walz, J. Phys.: Condens. Matter **14**, R285 (2002).
[7] S. K. Arora, H.-C. Wu, R. J. Choudhary, I. V. Shvets, O. N. Mryasov, H. Yao, and W. Y. Ching, Phys. Rev. B **77**, 134443 (2008).
[8] D. T. Margulies, F. T. Parker, F. E. Spada, R. S. Goldman, J. Li, R. Sinclair, and A. E. Berkowitz, Phys. Rev. B **53**, 9175 (1996).
[9] S. Kale *et al.*, Phys. Rev. B **64**, 205413 (2001).
[10] W. Eerenstein, T. T. M. Palstra, T. Hibma, and S. Celotto, Phys. Rev. B **68**, 014428 (2003).
[11] R. G. S. Sofin, S. K. Arora, and I. V. Shvets, J. Appl. Phys. **97**, 10D315 (2005).
[12] W. Eerenstein, T. T. M. Palstra, S. S. Saxena, and T. Hibma, Phys. Rev. Lett. **88**, 247204 (2002).
[13] S. K. Arora, R. G. S. Sofin, and I. V. Shvets, Phys. Rev. B **72**, 134404 (2005).
[14] J. Smit, Physica (Amsterdam) **17**, 612 (1951).
[15] T. R. McGuire and R. I. Potter, IEEE Trans. Magn. **11**, 1018 (1975).
[16] J. P. Jan, in *Solid State Physics*, edited by F. Seitz and D. Turnbull (Academic, New York, 1957), Vol. 5, p. 1.
[17] L. Berger, Physica (Amsterdam) **30**, 1141 (1964).
[18] R. I. Potter, Phys. Rev. B **10**, 4626 (1974).
[19] I. A. Campbell, A. Fert, and O. Jaoul, J. Phys. C **3**, S95 (1970).
[20] I. Pallecchi, A. Gadaleta, L. Pellegrino, G. C. Gazzadi, E. Bellingeri, A. S. Siri, and D. Marré, Phys. Rev. B **76**, 174401 (2007).
[21] V. S. Amaral, A. A. C. S. Loureço, J. P. Araújo, A. M. Pereira, J. B. Sousa, P. B. Tavares, J. M. Vieira, E. Alves, M. F. da Silva, and J. C. Soares, J. Appl. Phys. **87**, 5570 (2000).
[22] K. I. Bolotin, F. Kuemmeth, and D. C. Ralph, Phys. Rev. Lett. **97**, 127202 (2006).
[23] C. Ruster, C. Gould, T. Jungwirth, J. Sinova, G. M. Schott, R. Giraud, K. Brunner, G. Schmidt, and L. W. Molenkamp, Phys. Rev. Lett. **94**, 027203 (2005).
[24] M. Viret, M. Gabureac, F. Ott, C. Fermon, C. Barreteau, G. Autes, and R. Guirado-Lopez, Eur. Phys. J. B **51**, 1 (2006).
[25] M. Bibes, V. Laukhin, S. Valencia, B. Martínez, J. Fontcuberta, O. Y. Gorbenko, A. R. Kaul, and J. L. Martínez, J. Phys.: Condens. Matter **17**, 2733 (2005).
[26] M. Ziese and H. J. Blythe, J. Phys.: Condens. Matter **12**, 13 (2000).
[27] S. Sena, R. Lindley, H. Blythe, C. Sauer, M. Al-Kafarji, and G. Gehring, J. Magn. Magn. Mater. **176**, 111 (1997).
[28] S. K. Arora, R. G. S. Sofin, I. V. Shvets, R. Kumar, M. W. Khan, and J. P. Srivastava, J. Appl. Phys. **97**, 10C310 (2005).
[29] M. Ziese and C. Srinitiwarawong, Phys. Rev. B **58**, 11519 (1998).
[30] N. F. Mott, *Conduction in Non-Crystalline Materials* (Clarendon, Oxford, 1993), p. 17ff.
[31] S. B. Ogale, K. Ghosh, R. P. Sharma, R. L. Greene, R. Ramesh, and T. Venkatesan, Phys. Rev. B **57**, 7823 (1998).
[32] D. Ihle and B. Lorenz, J. Phys. C **19**, 5239 (1986).
[33] M. Ziese, Phys. Rev. B **62**, 1044 (2000).
[34] X. Jin, R. Ramos, Y. Zhou, C. McEvoy, and I. V. Shvets, J. Appl. Phys. **99**, 08C509 (2006).
[35] J. O'Donnell, J. N. Eckstein, and M. S. Rzchowski, Appl. Phys. Lett. **76**, 218 (2000).
[36] D. Wu, P. Wei, E. Johnston-Halperin, D. D. Awschalom, and J. Shi, Phys. Rev. B **77**, 125320 (2008).
[37] A. W. Rushforth, K. Vyborny, C. S. King, K. W. Edmonds, R. P. Campion, C. T. Foxon, J. Wunderlich, A. C. Irvine, P. Vasek, V. Novak, K. Olejnik, J. Sinova, T. Jungwirth, and B. L. Gallagher, Phys. Rev. Lett. **99**, 147207 (2007).
[38] M. Bibes, B. Martínez, J. Fontcuberta, V. Trtik, C. Ferrater, F. Sánchez, M. Varela, R. Hiergeist, and K. Steenbeck, J. Magn. Magn. Mater. **211**, 206 (2000).
[39] W. Döring, Ann. Phys. **424**, 259 (1938).
[40] R. P. vanGorkom, J. Caro, T. M. Klapwijk, and S. Radelaar, Phys. Rev. B **63**, 134432 (2001).
[41] R. R. Birss, *Symmetry and Magnetism* (North-Holland, Amsterdam, 1964).
[42] P. A. A. van der Heijden, M. G. van Opstal, C. H. W. Swüste, P. H. J. Bloemen, J. M. Gaines, and W. J. M. de Jonge, J. Magn. Magn. Mater. **182**, 71 (1998).
[43] C. Boekema, R. L. Lichti, A. B. Denison, A. M. Brabers, D. W. Cooke, R. H. Heffner, R. L. Hutson, and M. E. Schillaci, Hyperfine Interact. **31**, 487 (1986).
[44] S. M. Shapiro, M. Iizumi, and G. Shirane, Phys. Rev. B **14**, 200 (1976).
[45] Y. Yamada, N. Wakabayashi, and R. M. Nicklow, Phys. Rev. B **21**, 4642 (1980).
[46] D. Ihle, Z. Phys. B: Condens. Matter **58**, 91 (1985).
[47] P. Piekarz, K. Parlinski, and A. M. Olés, Phys. Rev. Lett. **97**, 156402 (2006).
[48] P. Piekarz, K. Parlinski, and A. M. Olés, Phys. Rev. B **76**, 165124 (2007).
[49] I. V. Shvets, G. Mariotto, K. Jordan, N. Berdunov, R. Kantor, and S. Murphy, Phys. Rev. B **70**, 155406 (2004).
[50] R. J. McQueeney, M. Yethiraj, W. Montfrooij, J. S. Gardner, P. Metcalf, and J. M. Honig, Phys. Rev. B **73**, 174409 (2006).